ISSN: 2447-3359

REVISTA DE GEOCIÊNCIAS DO NORDESTE

Northeast Geosciences Journal

v. 8, nº 2 (2022)

https://doi.org/10.21680/2447-3359.2022v8n2ID19514

Petrophysical and mineralogical aspects of sedimentary rocks in the sousa formation, Rio do Peixe basin (PB)

Aspectos petrofísicos e mineralógicos de rochas sedimentares da formação sousa, bacia do Rio do Peixe (PB)

Francisco de Assis da Silveira Gonzaga[1]; Josenildo Isidro dos Santos Filho [2]; Joelson Souza Isidro dos Santos [3]; Guilherme dos Santos Teles[4]; Henrique Bruno Lima de Oliveira[5]

[1] Federal Institute of Paraíba, Campina Grande campus, Campina Grande/PB, Brasil. E-mail: franciscoagonzaga@hotamail.com
ORCID: https://orcid.org/0000-0002-6975-0315

[2] Federal University of Campina Grande, Unidade Acadêmica de Mineração e Geologia, Campina Grande/PB, Brasil. E-mail: josenildoisidro@gmail.com
ORCID: https://orcid.org/0000-0001-6307-8057

[3] Federal University of Campina Grande, Unidade Acadêmica de Engenharia Agrícola, Campina Grande/PB, Brasil. E-mail: joelsonisidro700@gmail.com
ORCID: https://orcid.org/0000-0001-5563-0892

[4] Federal University of Campina Grande, Unidade Acadêmica de Mineração e Geologia, Campina Grande/PB, Brasil. E-mail: guilherme.santos@professor.ufcg.edu.br
ORCID: https://orcid.org/0000-0002-0615-8373

[5] Federal Institute of Paraíba, Campina Grande campus Campina Grande/PB, Brasil. E-mail: henriquuebruno@gmail.com
ORCID: https://orcid.org/0000-0002-9789-8923

Abstract: The Rio do Peixe Basin, Northeastern Brazil, is an important intracontinental basin that has aroused the interest of the oil industry and the scientific community due to the identification of an oil system. In this context, rocks from the Sousa Formation presented a great potential for the generation of hydrocarbons. However, confirmation of the potential for exploration of hydrocarbons and basin depends on more detailed studies of the permo-porous characteristics of generators and reservoirs. In this sense, the present work deals with the identification of petrophysical properties of four types of sedimentary rocks (shales, sandstones and siltstones) that are representative of the Sousa Formation. The were identified for analysis of structuring analysis for characterization of internal identification (porosity and permeability) and X-ray diffractometry (XRD) for the mineralogy. As tomcollation images were made in Avizo Fire® software, through the three-dimensional representation of the porosities of the rock blocks and simulation of fluid perfusion. Mineralogical data point to the presence of carbonates in the rocks, mainly calcite and lomite. The tomographic analysis indicates the porosity of the blocks ranging from 0.44% (red shale) to 6.09% (green shale). The permeability quantification ranges from 0.0043mD (red sandstone) to 4.6234mD (siltite) for a used observation scale. The porosity and permeability values found may be related to different diagenetic processes among the observed lithologies.

Keywords: Petrophysics; Sedimentary rocks; Rio do Peixe Basin.

Resumo: A Bacia do Rio do Peixe, Nordeste do Brasil, é uma importante bacia intracontinental que tem despertado o interesse da indústria petrolífera e da comunidade científica devido à identificação de um sistema petrolífero. Neste contexto, as rochas da Formação Sousa apresentaram um grande potencial para a geração de hidrocarbonetos. No entanto, a confirmação do potencial de exploração de hidrocarbonetos na bacia depende de estudos mais detalhados das características permo-porosas dos potenciais geradores e reservatórios. Nesse sentido, o presente trabalho trata da identificação das propriedades petrofísicas de quatro tipos de rochas sedimentares (folhelhos, arenitos e siltitos) representativas da Formação Sousa. As amostras foram submetidas à análise tomográfica para identificação da estrutura interna (porosidade e permeabilidade) e difratometria de raios X (DRX) para caracterização mineralógica. As imagens tomográficas foram analisadas no software Avizo Fire®, por meio da reconstrução tridimensional das porosidades dos blocos rochosos e da simulação de percolação de fluido. Dados mineralógicos indicam a presença de carbonatos nas rochas analisadas, principalmente calcita e dolomita. A análise tomográfica indica a porosidade dos blocos variando de 0,44% (folhelho vermelho) a 6,09% (folhelho verde). A quantificação da permeabilidade variou de 0,0043mD (arenito vermelho) a 4,6234mD (siltito) para a escala de observação utilizada. Os valores de porosidade e permeabilidade encontrados podem estar relacionados a diferentes processos diagenéticos entre as litologias observadas.

Palavras-chave: Petrofísica; Rochas sedimentares; Bacia do Rio do Peixe.

Received: 17/12/2019; Accepted: 03/09/2021; Published: 23/09/2022.

1. Introduction

The Rio do Peixe Basin (BRP) is an important intracontinental sedimentary basin located in the Northeast Region of Brazil, situated on the boundaries between the states of Ceará and Paraíba. Like other inland basins in the region, the BRP was formed by the crustal stretching process responsible for the fragmentation of Gondwana during the Early Cretaceous (Françolin et al., 1994). The BRP covers a total area of approximately 1250 km2, and is subdivided into three sedimentary sub-basins: (1) Brejo das Freiras, (2) Sousa, and (3) Pombal, separated by the basement heights of the Borborema Province (Françolin et al. al., 1994; Nogueira et al., 2004; Vasconcelos et al., 2020). The largest of the sub-basins is Sousa, with about 675 km2, followed by Brejo das Freiras, with 500 km^2, and Pombal, with approximately 75 km2 (Matos et al. 2016).

The rifite section of the BRP is divided into three formations that make up the Rio do Peixe Group (Figure 1): Antenor Navarro, Sousa Formation, Rio Piranhas, which are predominantly composed of terrigenous continental sediments of fluvio-lacustrine origin, deposited during the Lower Cretaceous (145-100 Ma; Córdoba et al., 2008; Rapozo et al., 2021).

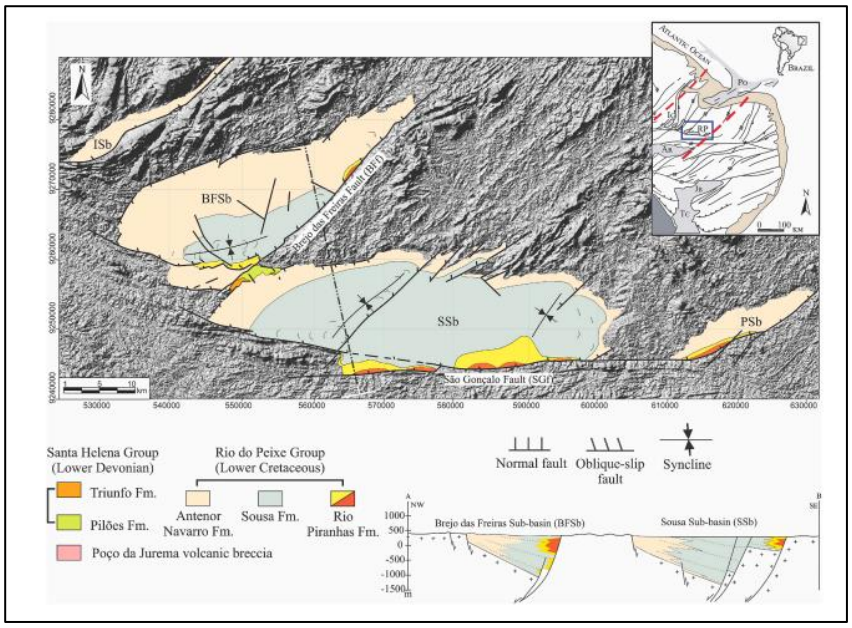

Figure 1 – Simplified geological sketch of the Rio do Peixe Basin, the red rectangle indicates the location of the study area.
Source: Modified from Rapozo et al. (2021).

The Antenor Navarro Formation consists of conglomerates and conglomeratic (immature) sandstones with medium-sized and tabular cross-bedding channels, ranging in color from cream to reddish (Córdoba et al., 2008; Medeiros, 2008). Medium to fine sandstone levels are present, which occur more sporadically towards the top of the sequence. The facies association of this unit is representative of alluvial fans and intertwined river systems (Rapozo et al., 2021).

The Sousa Formation is characterized by shales and siltstones interspersed with sandstones, which indicate sedimentation in a lacustrine environment influenced by ephemeral drainages (Rapozo et al., 2021). The siltstones and shales are reddish and locally grey-green, laminated, with wavy marks, contraction cracks and subordinate carbonate levels (Silva, 2009). Finally, the Rio Piranhas Formation, in turn, is composed of fine to coarse sandstones with cross bedding, with interspersed pebbles, in addition to coarse sandstones and supported matrix conglomerates (Córdoba et al., 2008; Medeiros, 2008), which represent alluvial fan systems associated with braided rivers (Rapozo et al., 2021).

The Rio do Peixe Basin has aroused the interest of the oil industry and the scientific community for the identification of an oil system in the basin (Fontes, 2007), with rocks from the Sousa Formation presenting great potential for hydrocarbon generation (Fernandes et al., 2017) . However, confirmation of the potential for hydrocarbon exploration in the basin depends on more detailed studies of the permo-porous characteristics of potential generators and reservoirs.

The characteristics of sedimentary rocks, such as porosity and permeability, as explained by Gonzaga (2018), differ for each lithogy observed, depending on the texture and structure present in the rock, in addition to the existing cement and its

distribution along the rocky body, structural aspects such as of compaction and fracturing of the massif. Rodrigues (2018) explains that favorable rocks for the formation of an unconventional reservoir system, where the rock structure that generates the fluid is the same that stores it, represent important producing rocks in interior sedimentary basins, with the BRP rocks, especially those corresponding to the Sousa Formation, included in this category.

Currently, the use of simple and non-destructive methods, such as computed tomography, allow the assessment of the degree of porosity and the presence of permeability in sedimentary rocks with greater precision and speed (Porto, 2015; Gonzaga, 2017; Rodrigues, 2018). This technique is capable of qualitatively distinguishing small density differences in the analyzed sample. The information, obtained through the emission of x-rays, by means of scanning at different angles and with continuous frequency, is applied to the study of sedimentary rocks, to identify the behavior of internal structures and to assess the rock's ability to carry fluids on smaller scales. (Porto, 2015; Rodrigues, 2018) and older (Gonzaga, 2017). After the internal imaging, the use of software enables the reconstruction of two- and three-dimensional models, representing approximate results of petrophysical (porosity and permeability) and morphological aspects, such as pore shape and distribution.

Due to the identification of a petroleum system in the Rio do Peixe Basin, in which the Sousa Formation has a good generating potential, this work evaluated the petrophysical (porosity and permeability) and mineralogical properties of representative rocks of the formation, using the tomography technique. computed tomography and X-ray diffractometry (XRD) analysis.

2. Methodology

Four samples of shales, sandstones and siltstones, characteristic of the Sousa Formation, were collected. Measurements of lodging and discontinuity families were performed in the outcrops visited. For tomographic analyses, the samples were cut into blocks of approximately 6.0 x 6.0 x 3.0 cm (Figure 2-A), then the blocks received an arrow to indicate the stratigraphic top of the sample (Figure 2 -Ç). For the X-ray diffraction analysis, the samples were macerated to suit the granulometry in approximately 200 mesh (Figure 2-D).

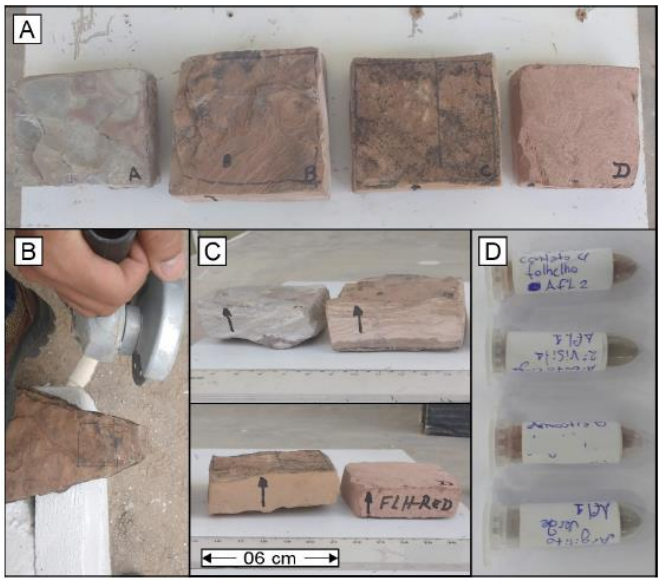

Figure 2 – In (A) Rock blocks from left to right: greenish shale, red shale, siltstone and red sandstone. (B) Use of an angle grinder to cut the collected samples, in order to reduce them into blocks of approximately 6.0 x 6.0 x 3.0 cm. (C) Blocks of rocks with arrow indicating stratigraphic top. (D) Macerated samples with a granulometry of approximately 200 mesh for XRD analysis.
Source: Authors, 2019.

The sample blocks were taken to the Dom Luiz Gonzaga Fernandes Emergency and Trauma Hospital in Campina Grande-PB, where their internal imaging was performed using a 64-channel Phillips Brilliance tomography device. To

obtain the images, the following standards were used, according to the methodological sequence proposed by Gonzaga (2017): slice of 0.7 mm, scan time of 05 seconds, increment of 0.5 mm, filter dedicated to bone human, field size used (FOV) of 200 mm and matrix of 1024 x 1024 pixels (high resolution). The imaging process starts with the table advancing towards the gantry, which emits X-radiation. The rays are attenuated when they come into contact with the rock block and are captured by detectors. Then, the data acquisition system receives the processed information and generates images (slices) that were later processed in the Avizo Fire® software, where it was possible to reconstruct three-dimensional images of the samples.

The macerated samples (Figure 2-D) were taken to the Laboratory of Evaluation and Development of Biomaterials in the Northeast - CERTBIO, located at the Federal University of Campina Grande (UFCG), where they were analyzed using the X-ray Diffractometry (XRD) technique. use of diffractometer model SHIMADZU – XRD-7000.

2.1. Digital Image Processing (PDI)

To facilitate the interpretation of the porosity of the samples analyzed by computed tomography, contrast was applied to the images generated by the Avizo Fire® software. All images received the same amount of contrast.

The identification of the porosity of the blocks occurred from the processing of the slices obtained by computed tomography in Avizo Fire®. From this, it was possible to reconstruct the three-dimensional samples and visualize the structural properties of the different rocks. Figure 3 presents the methodological sequence used in the software to build a three-dimensional model of pore spaces and quantify the volume of pores in the sample.

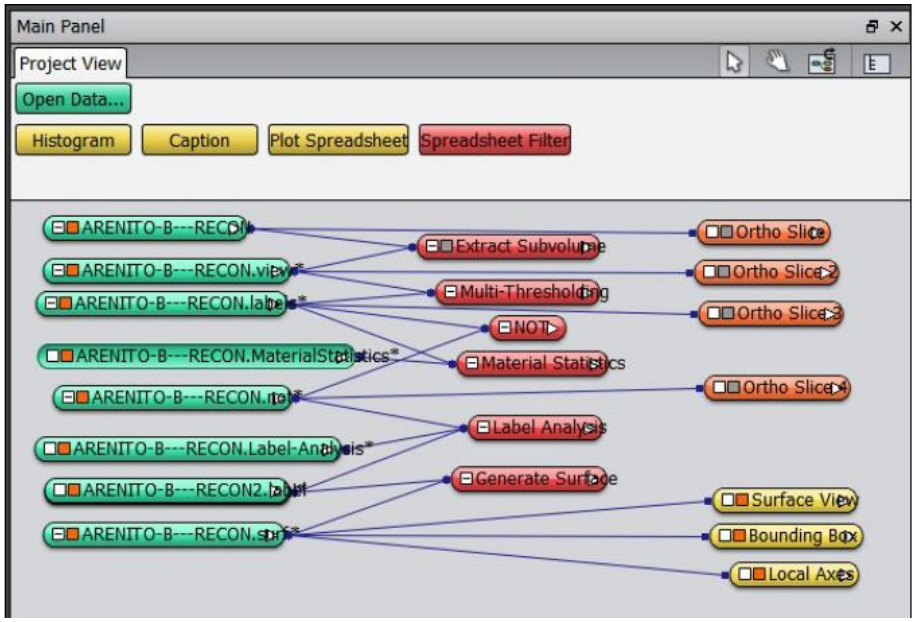

Figure 3 – Methodological sequence applied using the Avizo Fire® software to obtain a three-dimensional model and quantify the effective porosity of the samples.
Source: Authors, 2019.

To obtain the three-dimensional model of the pores of the samples and their quantification, the set of tomographic images (slices) must be inserted in the software, in the option “Open Data...” (Figure 3). the “Ortho Slice” visualization tool is applied (Figure 4). During the procedure, you can extract the desired information from a specific part of the slice, delimiting the selected sample area, this is possible using the "Extract Subvolume" option. Avizo Fire®, through the "Multi-Threshold" option, makes use of the color difference of the pixels of the slices to identify and separate the components of the rock framework. In this case, the densest constituents appear in lighter gray tones, while the porous spaces (with lower density) appear in shades of dark gray/black (Rodrigues, 2018). In addition, the software makes it possible to quantify the volume of pore spaces (Vp), calculated by the ratio of pore volume/total volume, resulting in the effective porosity of the sample.

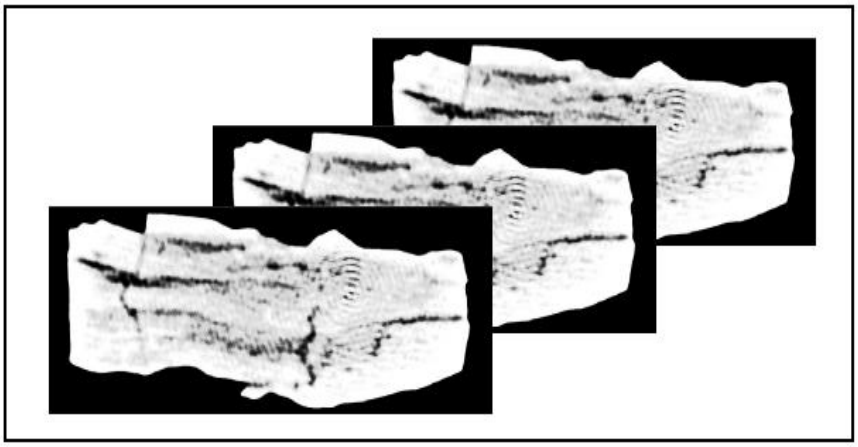

Figure 4 – Standardized image illustrating the processing of slices through the methodology used by the Avizo Fire® software.
Source: Authors, 2019.

To calculate the permeability in the samples, the same subvolume is used, delimited for the porosity calculation. However, the operational procedure shown in Figure 5 is used. Once the subvolume is delimited, the Resample tool is used to increase the resolution of the generated block. After segmenting the block images using the Interactive Thresholding tool, the Absolute Permeability Simulation tool is used, responsible for simulating the passage of a fluid through the z direction of the volume delimited by the analyzed block. The result of this tool is given in a table, in Darcy unit.

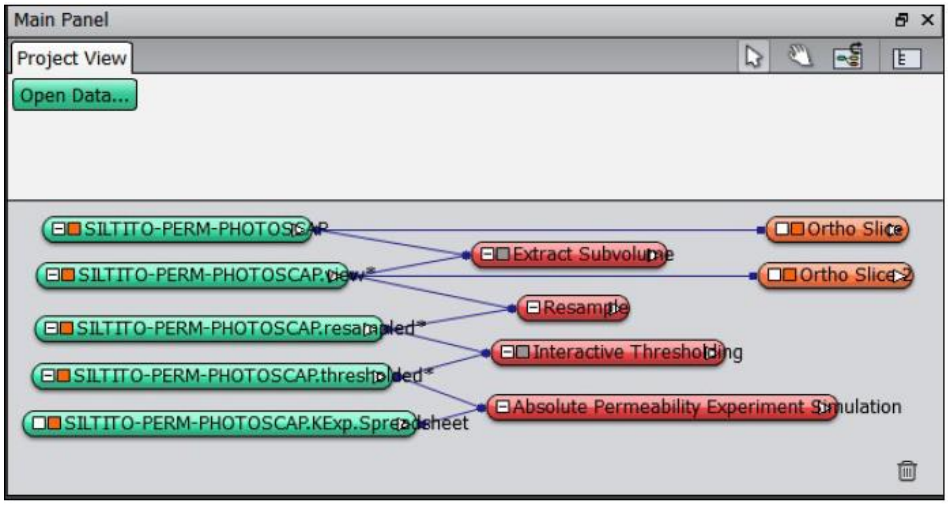

Figure 5 – Sequence applied using the Avizo Fire® software, to quantify the permeability of the samples.
Source: Authors, 2019.

3. Results and discussions

The observed outcrops showed families of discontinuities oriented preferentially to the NW-SE, according to the stereogram shown in Figure 6. The presence of discontinuities at the outcrop scale also demonstrates an influence on the permeability of the rocks. These discontinuities contribute to the primary porosity connection, allowing greater integration between the voids. The discontinuities observed in the studied outcrops are divergent, with respect to the directions of the Patos Shear Zone (W-E) and Portalegre Shear Zone (NE-SW), active in the border region of the study area. However, as observed by Córdoba et al. (2008) and Silva (2009), fractures with NW-SE orientation are common in the BRP.

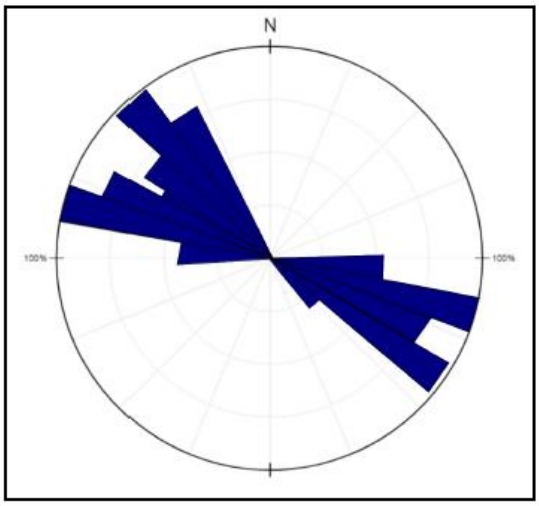

Figure 6 – Diagram of rosettes representing the fracture families observed in outcrops in the field.
Source: Authors, 2019.

XRD analyzes made it possible to identify the constituent minerals of the green shale, red shale, siltstone, and red sandstone samples (Figure 7). Among the minerals identified are dolomite, anorthite and calcite, for green shale; anorthite, calcite and quartz, in red shale; peaks for quartz, sandstone and calcite for sandstone and quartz, albite and calcite for siltstone.

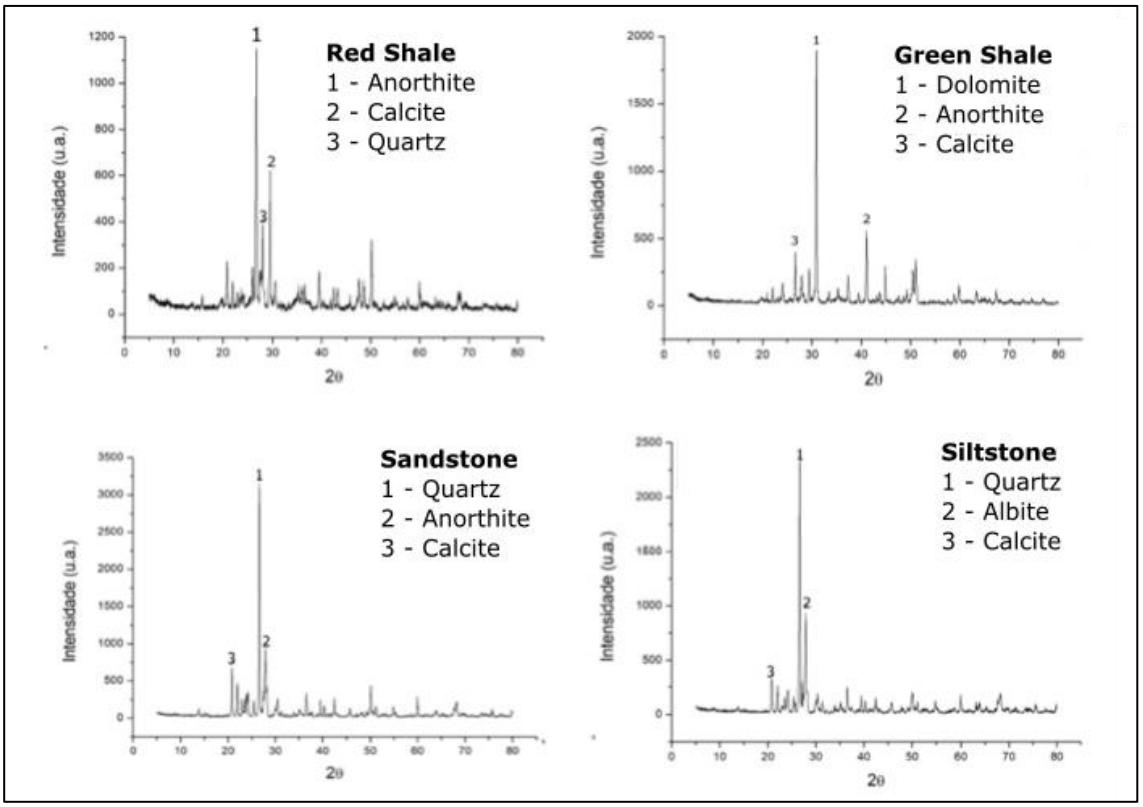

Figure 7 – X-ray diffractograms of the analyzed samples.
Source: Authors, 2019.

The greenish shale sample shows primary porosity, occurring parallel to the rock layers (Figure 8), which suggests its formation during the deposition of the layers. Fractures are also present in the sample, which occur perpendicular to the bedding (Figure 8), which suggests a process of secondary porosity formation originated by local tectonics.

These fractures behave like channels, connecting the parallel pores, favoring the flow of fluid inside the sample. In this case, according to the classification by Ahr (2008), the rock presents hybrid porosity, due to the distinction of primary pores, generated during deposition, and secondary pores, resulting from subsequent fracturing. Although the primary aspects are dominant in the sample, the secondary aspects are essential, acting as an active connection channel between the pores, considerably increasing the permeability in the rock.

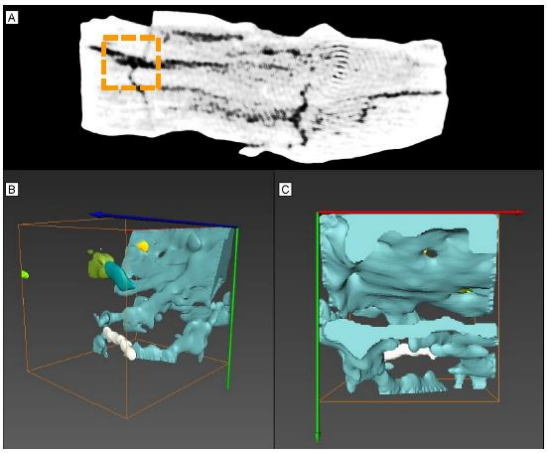

Figure 8 – (A) Tomographic image in the xy plane of the green shale, with delimitation (in orange) of the analyzed subvolume. (B) Three-dimensional block of the identified pore volume (fancy colors). (C) View of the block in the x(red) y(green) plane (fancy colors).
Source: Authors, 2019.

The red shale sample is characterized by elongated porous bodies (Figure 9-A), which accompany the bedrock, suggesting its primary (depositional) origin. However, unlike the previous sample, the pores of this sample do not have connectivity (Figure 9-B and C), which reduces their permeability.

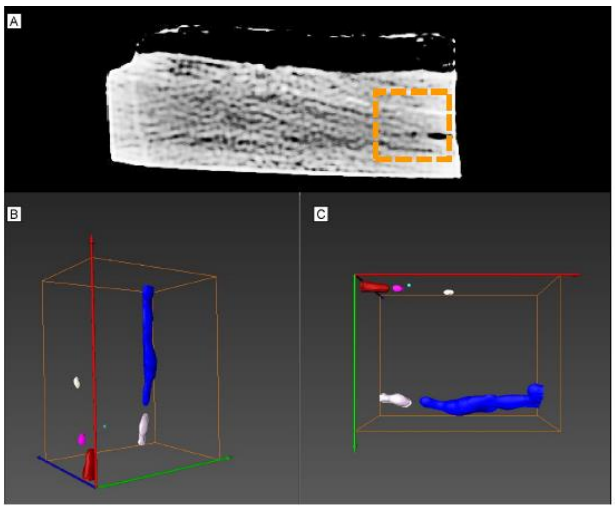

Figure 9 – (A) Tomographic image of the red shale, with delimitation (in orange) of the analyzed subvolume. (B) Three-dimensional block of identified porosity (fancy colors). (C) View of the block in the xy plane (fancy colors).
Source: Authors, 2019.

The pores observed in the siltstone sample can be observed elongated, in the plane formed by the xy axes (green and red, respectively), perpendicular to the bedding plane, along which stretched interconnected pores occur (Figure 10). However, this connectivity is not effective in the entire sample, in which isolated porous bodies dominate.

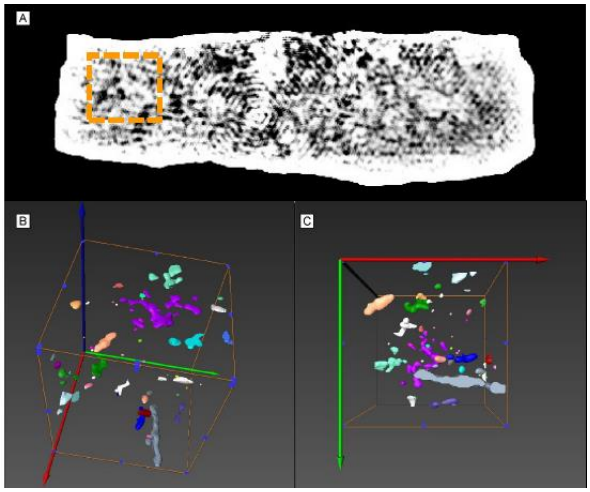

Figure 10 – (A) Tomographic image of the siltstone, with delimitation (in orange) of the analyzed subvolume. (B) Three-dimensional block of identified porosity (fancy colors). (C) View of the block in the xy plane (perpendicular to the bedding), in fancy colors.
Source: Authors, 2019.

The sandstone sample, in Figure 11, is characterized by the presence of small planar arrangements and intergranular spaces, filled with carbonate material, distributed throughout the analyzed block. Centimetric fractures occur on the diagonal of the highlighted face of the sample (Figure 11-A), representing a significant majority of the effective porosity present. Filled fractures and partially filled spaces represent natural blockages, contributing to the reduction of porosity and, consequently, of permeability in the sample. The presence of this filling material may result from the dissolution of carbonate cement existing between the quartz and feldspar grains that make up the sandstone.

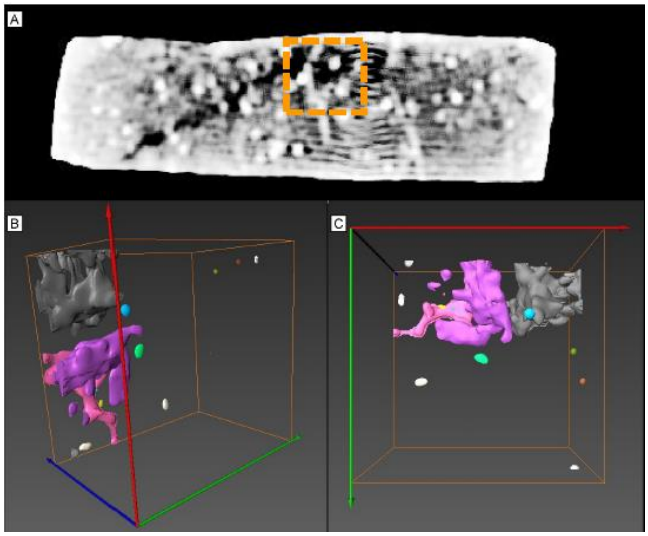

Figure 11 – (A) Tomographic image of the sandstone, with delimitation (in orange) of the analyzed subvolume. (B) Three-dimensional block of identified porosity (fancy colors). (C) View of the block in the xy plane (fancy colors).
Source: Authors, 2019.

Table 1 brings together the percentages of porosities (φ) and permeabilities of the analyzed rocks, determined by Avizo Fire®, highlighting the porosity (φ) in the value of 6.09% presented by the green shale block, which is the highest value obtained between the analyzed rocks and 0.44% in the red shale block, exemplifying the anisotropy characteristic among the BRP rocks.

Table 1 – Values in percentage of porosity (φ) and permeability (mD) of the analyzed rock blocks, simulated in Avizo Fire® software.

Sample	Porosity (%)	Permeability (mD)
Green Shale	6,09	0,0072
Red Shale	0,44	0,0094
Siltstone	1,59	4,6234
Sandstone	1,72	0,0043

Source: Authors, 2019.

The three-dimensional reconstruction of the samples allowed the measurement of existing porosity and permeability in each observed subvolume. Through the obtained data, the internal structures present in the samples were evaluated, in order to relate the existing porosities to the mineralogical aspects and fracture development. After generating the three-dimensional structures, it was possible to quantify the porosity present through the ratio of the proportion between the volume of pores and the total volume of each sample. The calculation of porosity and permeability through the generation of 3D images of the internal structure of the samples submitted to tomographic devices indicate porosity of the blocks ranging from 0.44% (red shale) to 6.09% (green shale). The quantification of permeability ranged from 0.0043 mD (red sandstone) to 4.6234 mD (siltite).

The three-dimensional reconstruction of the samples allowed the measurement of existing porosity and permeability in each observed subvolume. Through the obtained data, the internal structures present in the samples were evaluated, in order to relate the existing porosities to the mineralogical aspects and fracture development. After generating the three-dimensional structures, it was possible to quantify the porosity present through the ratio of the proportion between the volume of pores and the total volume of each sample. The calculation of porosity and permeability through the generation of 3D images of the internal structure of the samples submitted to tomographic devices indicate porosity of the blocks ranging from 0.44% (red shale) to 6.09% (green shale). The quantification of permeability ranged from 0.0043 mD (red sandstone) to 4.6234 mD (siltite).

The interplanar porosity, observed in the green shale, may be related to the lower degree of rock compaction, reflected in the percentage of porosity found between portions of the bedding. Although a primary porosity with larger dimensions is observed, the low permeability, for the observation scale, is in agreement with what is commonly found in these rocks. Red shale has low porosity and consequent permeability, which may be related to a higher degree of rock compaction, reducing empty spaces in the bedding.

Contrary to what is commonly observed in various types of sandstones, the sandstone sample evaluated presents reduced values for porosity and permeability, which may be related to the precipitation of cement (siliceous or carbonate) in the BRP sandstones, as described by Palhano (2021) in sandstones of the Antenor Navarro Formation. The siltstone, despite having small pores distributed within the sample, has a high permeability, suggesting that they are pores connected throughout the evaluated volume.

4. Final considerations

The use of computed tomography presents contributions to the petrophysical evaluation of sedimentary rocks, however, the low resolution of the generated images does not allow the identification of smaller pores, being limited only to macroporosity. For the observation scale used, the low porosity and permeability values indicate that the analyzed samples do not present favorable conditions to be classified as reservoir rock.

The characterization of samples at different scales of observation, such as microtomography, associated with laboratory analysis, through equipment such as gas permoporosimeter and microscopic petrography, is necessary to verify if the petrophysical aspects identified through tomography are maintained. if constant on smaller scales.

It is recommended, for future work, more detailed and refined chemical analyses, including the quantification of Total Organic Carbon (TOC), CO_2 and hydrogen and oxygen indices in amorphous materials, as these compounds are related to

the indication of occurrences of hydrocarbons. The results indicated by the percentage of porosity present in the green shale, can configure a perspective of more detailed studies about the shales of the region, with special attention to the richest in carbonates, because these rocks are considered potential unconventional reservoirs.

Acknowledgment

The authors express their thanks to the IFPB Campina Grande, for their constant efforts in scientific research, as well as to the reviewers and evaluators for the corrections and suggestions given to this work.

References

AHR, W.; M. *Geology of carbonate resevoirs: the identification, description, and characterization of hidrocarbon reservoirs in carbonate rocks*. New Jersey, USA: John Wiley & Sons. P. 277, 2008.

CÓRDOBA, V. C.; ANTUNES, A. F.; JARDIM DE SÁ, E. F., NUNES DA SILVA, A.; SOUSA, D. C.; LINS, F. A. P. L. *Análise estratigráfica e estrutural da Bacia do Rio do Peixe Nordeste do Brasil: integração de dados a partir do levantamento sísmico pioneiro 0295_rio_do_peixe_2d*. Boletim de Geociências da Petrobras, 16 (1): 53-68. 2017.

FERNANDES, Y. L.; MUNIZ, Y. M.; JUNIOR, N. J. R. C. *Avaliação do Potencial Gerador da Formação Sousa, Bacia do Rio Do Peixe, Utilizando Dados de Pirólise Rock-Eval e Carbono Orgânico Total*. X Simpósio Sul Brasileiro de Geologia. Curitiba (2017).

FRANÇOLIN, J.B.; COBBOLD, P.R.; SZATMARI, P. 1994. Faulting in early Cretaceous Rio do Peixe basin (NE Brazil) and its significance for the of the Atlantic openning. J. Struc. Geol., 16(5): 647-661.

GONZAGA, F. A. S. *Caracterização petrofísica multiescalar de tufas carbonáticas da Formação Jandaíra, Bacia Potiguar* – Campina Grande, 2017. Tese (Doutorado em Engenharia de Processos) – Universidade Federal de Campina Grande, Centro de Ciências e Tecnologia, 2017.

MATOS, T.R.B.; NORMANDO, L.C.; ALMEIDA, L. R. B.; SOARES, J. A. *Análise das Propriedades Petrofísicas das Rochas Sedimentares da Bacia Rio do Peixe*. II Congresso Nacional De Engenharia de Petróleo, Gás Natural e Biocombustíveis e IV Workshop de Engenharia de Petróleo. Natal – RN. 2016.

MEDEIROS, V.C. (Org). *Geologia e Recursos Minerais da Folha Sousa SB.24-X-A. Escala 1:250.000*. Estados da Paraíba, Rio Grande do Norte e Ceará. 312p. Recife: CPRM – Serviço Geológico do Brasil, 2008.

NOGUEIRA, F. C. C., OLIVEIRA, M. S. de, CASTRO, D.L. de; Estudo Magnético e Gravimétrico do Arcabouço Estrutural da Bacia Rio do Peixe-PB, Universidade Federal do Ceará, Revista de Geologia, vol.17, n 1, 74-87, 2004.

PALHANO, L. C. *Influência Da Silicificação Hidrotermal Nas Propriedades Físicas De Arenitos Arcoseanos Afetados Por Zona De Falha, Bacia Rio Do Peixe, NE do Brasil.* Dissertação de Mestrado. Universidade Federal do Rio Grande do Norte, Centro de Ciências Exatas e da Terra. Programa de Pós-graduação em Geodinâmica e Geofísica. 2009.

RAPOZO, B. F.; CÓRDOBA, V. C.; ANTUNES, A. F. Tectono-stratigraphic evolution of a cretaceous intracontinental rift: Example from Rio do Peixe Basin, north-eastern Brazil. Marine and Petroleum Geology, vol. 126, n 1, 1-27, 2021.

PORTO, A. L. *Estimação de propriedades petrofisicas de rochas sedimentares a partir de imagens microtomográficas de Raios-X*. Tese (Doutorado em Engenharia de Processos) – Universidade Federal de Campina Grande, Centro de Ciências e Tecnologia, Campina Grande/PB. 2015.

RODRIGUES, I. S. *Caracterização Multiescalar Petrofísica e Mineralógica de Folhelhos da Bacia do Araripe*. Dissertação (Mestrado) – Programa de Pós Graduação em Exploração Petrolífera e Mineral – Universidade Federal de Campina Grande, Centro de Tecnologia e Recursos Naturais, 2018.

SILVA, A. N. *Arquitetura, Litofáceis e Evolução Tectonoestratigráfica da Bacia do Rio do Peixe, Nordeste do Brasil.* Dissertação de Mestrado. Universidade Federal do Rio Grande do Norte, Centro de Ciências Exatas e da Terra. Programa de Pós-graduação em Geodinâmica e Geofísica. 2009.

VASCONCELOS, D. L.; MARQUES, F. O.; NOGUEIRA, F. C. C.; PEREZ, Y. A. R.; BEZERRA, F. H. R.; STOHLER, R. C.; SOUZA, J.A.B. Tectonic inversion assessed by integration of geological and geophysical data: the intracontinental Rio do Peixe Basin, NE Brazil. Basin Research, 2020.